RESEARCH ARTICLE | JULY 03 2019

Synthesis, characterization and antibacterial activity of silver doped TiO_2 photocatalyst FREE

Nur Aini ✉; Saoki Rachman; Anik Maunatin; Aminatus Syarifah

AIP Conf. Proc. 2120, 050017 (2019)
https://doi.org/10.1063/1.5115693

Synthesis, Characterization and Antibacterial Activity of Silver Doped TiO_2 Photocatalyst

Nur Aini[1, a)], Saoki Rachman[1, b)], Anik Maunatin[1, c)] and Aminatus Syarifah[1, d)]

[1]*Energy and Environmental Research Group, Chemistry Departement, Universitas Islam Negeri Malang, Jl. Gajayana No.50 Malang, Indonesia*

[a)]Corresponding author: nuraini@kim.uin-malang.ac.id
[b)]saokirahman2@gmail.com
[c)]a_maunatin@yahoo.com
[d)]14630028@student.uin-malang.ac.id

Abstract. Silver was doped into TiO_2 semiconductor in order to improve the antibacterial activity of TiO_2 photocatalyst under ultraviolet and visible light radiation due to its ability to modify the band gap energy of TiO_2. Silver doped TiO_2 photocatalysts were successfully synthesized using the sonochemical method at various silver concentration i.e 1,3,5,7, and 9%. Structural studies from XRD data showed that either undoped and silver-doped TiO_2 crystallized in a single phase structure of anatase TiO_2 with $I4_1$/amd space group. UV-Vis Diffuse Reflectance spectra resulted in the bandgap energy of undoped and silver-doped TiO_2 were 3.4 eV, 3.0 eV, 3.3 eV, 3.1 eV, 3.25 eVand 2.8 eV respectively. Among those various dopant concentrations, 9% Ag-doped TiO_2 showed the highest decrease in reflectance and band gap energy. Antibacterial activity of all synthesized materials toward *E. coli* antibacterial activity achieved the highest value for 9% of silver-doped TiO_2 under ultraviolet and visible light irradiation. Zero viability occurred at 50mg/30mL of culture for 9% of Ag-doped TiO_2 under visible irradiation. Inhibition zone and viability test confirmed that Ag content plays a significant role in increasing the antibacterial activity of silver-doped TiO_2 photocatalyst.

INTRODUCTION

The anatase phase of titanium dioxide (TiO_2) is well known functional material with superior photocatalytic activity and stability toward organic pollutant degradation compared to the others phase of TiO_2 i.e rutile and brookite phase [1]. However, anatase phase TiO_2 can only active under ultraviolet (UV) radiation due to its wide band gap energy. Further modification by inserting various metal dopants into anatase phase lattice has been reported to enhance its photocatalytic activity into a wider spectrum in the visible region. Among transition metal dopant, silver doped TiO_2 has the potential to be developed as a functional material in environmental and industrial water purification. The silver metal itself has antibacterial activity against gram positive and negative bacteria [2-3]. Addition of silver as a metal dopant into anatase TiO_2 is expected to enhance not only its photocatalytic activity under visible light irradiation but also its antibacterial activity both under UV and visible region.

Various methods have been developed to synthesize metal-doped TiO_2 such as sol-gel methods and sonochemical method [4]. The sonochemical method employs ultrasonic wave radiation to provide a homogenous, simple and fast method in material synthesis. Ultrasonic wave irradiation exhibits a cavitation phenomenon [4] which provides high energy of active site in short reaction time. Cavitation properties of ultrasound radiation can produce a small particle size and large surface area of synthesized material which subsequently offer an advantage in photocatalytic and antibacterial activity.

International Conference on Biology and Applied Science (ICOBAS)
AIP Conf. Proc. 2120, 050017-1–050017-6; https://doi.org/10.1063/1.5115693
Published by AIP Publishing. 978-0-7354-1860-8/$30.00

EXPERIMENTAL DETAILS

Synthesis of Undoped and Silver Doped TiO_2 Photocatalyst

Undoped TiO_2 was synthesized using TTIP (titanium isopropoxide, Sygma Aldrich) as Ti precursor. 10 mL TTIP was added dropwise into 60 mL solution of ethanol:deionize water (3/1 v/v) [5]. This homogenous mixture transferred into the low intensity of ultrasonic cleaning bath and irradiated with ultrasonic wave for 1h. White precipitation was obtained and dried at 100˚C for about 2h. The dried sample ground, pressed into pellet then calcined at 450˚C for 2h. Silver doped material at various silver contents also synthesized using the same method with the addition the stoichiometric amount of silver nitrate into the homogenous mixture of TTIP-ethanol: deionized water. Silver was added into a homogenous mixture of TTIP in ethanol: deionized water at w/w of atomic ratios of Ag i.e 1,3, 5, 7, 9. Addition of silver resulted in grey to dark grey powder as increasing the silver concentration.

Characterization of Undoped TiO_2 and Silver Doped TiO_2 Photocatalyst

The phase structure of all photocatalyst materials was measured by Powder X-Ray Diffraction (XRD, XPert MPD Diffractometer) with Cu-Kα radiation at a scanned 2θ range of 5-90˚. Diffractogram data subsequently compared with ICSD (Inorganic Crystal Structure Database) standard for type phase of TiO_2 including anatase, rutile, and brookite phase. The crystallographic data of all synthesized material also determined by the refinement process using Le Bail Refinement Method of Rietica Program. The crystallite size of material were calculated from diffractogram data at the highest peak intensity using Debye Scherrer formula (Equation 1) whereas D is the average crystallite size (Å), K is the Scherrer constant (0.89), λ is the X-ray wavelength for Cu-Kα_1 radiation (1.5406 Å), θ is the diffraction angle at maximum intensity, and B is the Full Width at Half Maximum (FWHM) in radians.

$$D = \frac{K\lambda}{B\ cos\theta} \qquad (1)$$

The reflectance properties were carried out by UV-Vis Diffuse Reflectance spectroscopy (DRS, Shimadzu UV-2450) at a wavelength range of 100-900nm. The collected reflectance data (R) converted to Kubelka-Munk function F(R) $(1-R^2/2R)$ which is corresponding to the absorption properties of photocatalyst materials. The band gap energy value obtained from the threshold energy between $(F(R)h\nu)^{½}$ versus photon energy ($h\nu$). In additional data, the morphological photocatalyst and elemental analysis of silver content ware carried out by SEM-EDX for the highest activity photocatalyst obtained in this research.

Antibacterial Activity of Undoped TiO_2 and Ag Doped TiO_2 Photocatalyst

The antibacterial activity of undoped and Ag-doped TiO_2 photocatalysts was evaluated against gram-negative bacteria of *E. coli* culture. *E. coli* culture were grown on nutrient broth agar at 2% inoculums, incubated at 37 °C for 2h until 0.27 optical density (OD) was achieved. *E. coli* culture with 0.27 OD equivalent to $7.8x10^8$ *cfu*/mL and used in antibacterial activity test. The suspension of undoped and silver-doped TiO_2 was prepared by added 50mg of photocatalyst material into 30 mL of *E. coli* culture and stirred for 1 h under UV light and visible light irradiation (40 W). The viability of *E. coli* determined by Total Plate Count (TPC) method with the average number of colony forming unit in two repeated experiment. Viability (%) counted by equation 2. Antibacterial effect of photocatalyst itself without light irradiation was confirmed qualitatively by inhibition zone method at 20 mg photocatalyst over 10 mL culture.

$$Viability\ (\%) = \frac{(number\ of\ control\ bacteria - number\ of\ treated\ bacteria)}{number\ of\ control\ bacteria}\ x\ 100\ \% \qquad (2)$$

RESULT AND DISCUSSION

Structural Properties of Undoped and Silver Doped TiO_2 Photocatalyst

Structural character of all synthesized materials was studied from XRD data in Fig 1. XRD pattern of undoped and Ag-doped TiO_2 exhibited agreement pattern with anatase phase structure of TiO_2 standard (ICSD no. 159910). The silver phase was detected at $2\theta = 44.5^\circ$ for 5% Ag-doped TiO_2. Silver dopant has been reported to induce the phase transformation at high content dopant, high temperature, or may depend on the type of precursor and synthesis method. Mogal, S.I *et al.* [6] reported that Ag-doped TiO_2 at (0.75-3.5 % atom Ag) showed anatase phase characteristic at 400 ˚C and 500 ˚C, however a silver phase and rutil phase exhibited at a higher temperature (600˚C) for higher silver content (3.0 and 3.5%) along with anatase phase. Gupta *et al.* [7] reported the presence of silver-phase at low calcination temperature (450˚C for 0.5 h) using acid catalysed sol-gel process with titanium tetrabutoxide procursor at 3 and 7% of silver. Nugussie *et al.* [8] also confirmed the presence of silver-phase at lower temperature synthesis (450 ˚C for 4h) using $TiCl_4$ precursor via sol-gel process. In this research, synthesis of silver-doped TiO_2 was carried out at 450 ˚C for 2h and using TTIP as Ti-precursor via the sonochemical method and resulted in the anatase phase. No phase transformation founded at synthesis condition employed. Ultrasound wave irradiation used in this research expected to induces a homogenous mixture of the silver-Ti precursor at various concentrations so that silver dopant can homogenously be mixed into the anatase phase. However, 5% of Ag dopant resulted in low peak related to the silver phase which might be caused by inhomogenous mixture during the synthesis process. In other hand, no silver phase or anatase phase transformation were detected for 1, 3, 7 and 9% of Ag-doped TiO_2 photocatalyst, so it can be implied that silver was well doped into anatase lattice of TiO_2 at those materials. The presence of silver in materials can be observed directly using the color change on the obtained product. White powder of TiO_2 turn into greyish powder as increasing the silver content. Silver content confirmed with SEM-EDX data shown in Fig. 2. for 9% of Ag-doped TiO2 at 0.325 eV.

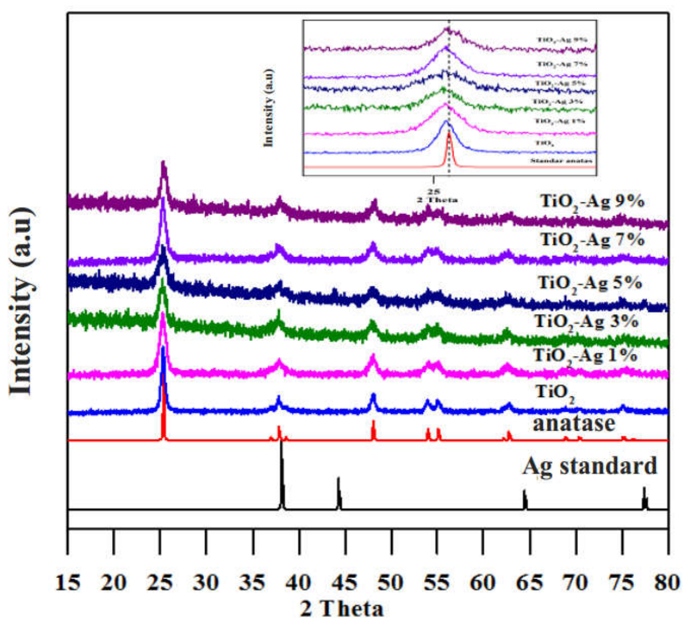

FIGURE 1. XRD Pattern of undoped and silver (Ag) doped TiO_2 photocatalyst at 1, 3, 5, 7, and 9% atomic ratio compared with Silver (Ag) Standart and Anatase phase of TiO_2

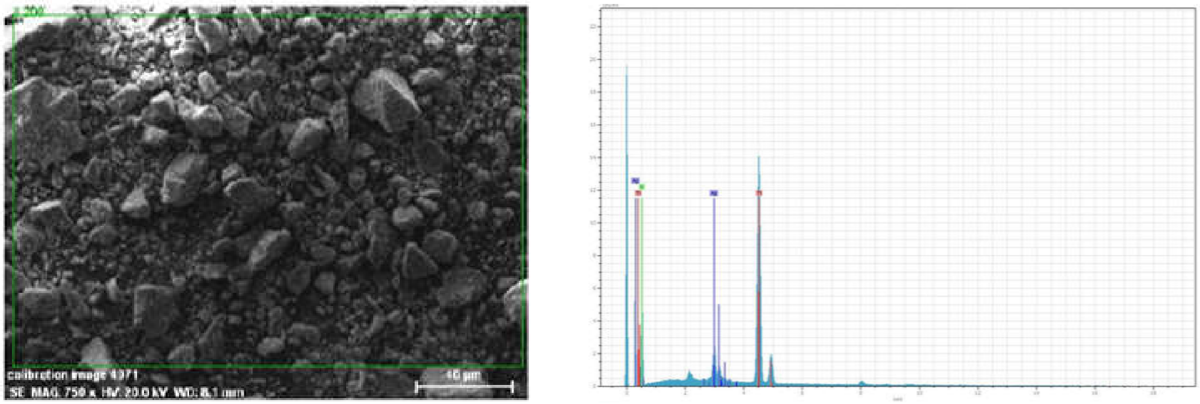

(a) (b)

FIGURE 2. SEM-EDX analysis for 9% of Ag-doped TiO_2 (a) Morphological surface measured by SEM (b) Elemental analysis

Further analysis on XRD pattern using Le Bail refinement, reveals that anatase phase in all series materials crystallized in a tetragonal lattice with $I4_1/amd$ space group and 4 asymmetric unit (Z). No significant alteration detected on the crystal lattice parameter and crystal volume. Crystallite size of all synthesized photocatalysts was determined by Debye Scherrer formula and listed in Table 1. All doped samples have smaller crystallite size than the undoped sample.

TABLE 1. Crystallite size of undoped and silver-doped photocatalyst calculated by Debye Scherrer formula

Photocatalyst Sample	The crystallite size (nm)
Undoped TiO_2	18.97
1% Ag-doped TiO_2	10.10
3% Ag-doped TiO_2	9.54
5% Ag-doped TiO_2	8.93
7% Ag-doped TiO_2	11.67
9% Ag-doped TiO_2	10.10

Optical Properties of Silver Doped TiO_2 Photocatalyst

Optical properties of undoped and doped TiO_2 determined from UV-Vis DRS measurement shown in Fig. 3. Reflectance data reveals that 9% of Ag-doped TiO_2 has the lowest decreasing in reflectance (Fig 3a) which is followed by the highest enhancement in visible absorption (Fig 3b). 9% Silver proved to increase absorption properties of anatase phase in the visible spectrum. Band gap energy of silver-doped TiO_2 photocatalysts was obtained from threshold energy in correlation curve between $(F(R)\ h\nu)^{1/2}$ versus energy ($h\nu$) (Fig 4). Indirect band gap energy of undoped TiO_2 and silver-doped TiO_2 (1-9%) were 3.4, 3.0, 3.3, 3.1, 3.25 and 2,8 eV. Decreasing bandgap energy only achieved 9% of the silver-doped photocatalyst. DRS data indicate that 9% of silver dopant will exhibit higher antibacterial activity than the composition of the other.

Antibacterial Activity of Silver Doped TiO_2

Antibacterial activity of silver-doped TiO_2 photocatalyst at various Ag concentration was tested against *E. coli* viability. Inhibition zone test was also employed as a qualitative test to know the antibacterial activity of all materials themselves without light irradiation at 20 mg photocatalyst over 10 mL culture. Undoped TiO_2, 1% Ag doped TiO_2 and 3% Ag doped TiO_2 does not shown inhibition zone against a colony of *E.coli*. In the other hand, 5, 7, and 9% Ag doped TiO_2 photocatalyst exhibited inhibition zone 4.9, 2.6 and 3.8mm respectively. Undoped and lower doped TiO_2 could not hindered the *E. coli* growth without light irradiation. However, at higher Ag concentration, silver doped TiO_2 can inhibits the E. coli growth. This evidence indicated that silver content plays an important role in antibacterial activity in the absence of light irradiation. The highest inhibition test was achieved for

5% of Ag doped TiO_2 which shown the silver phase content in its XRD pattern. Measured viability (%) of *E. Coli* under ultraviolet and visible light irradiation were listed in Table 2 and Table 3, respectively.

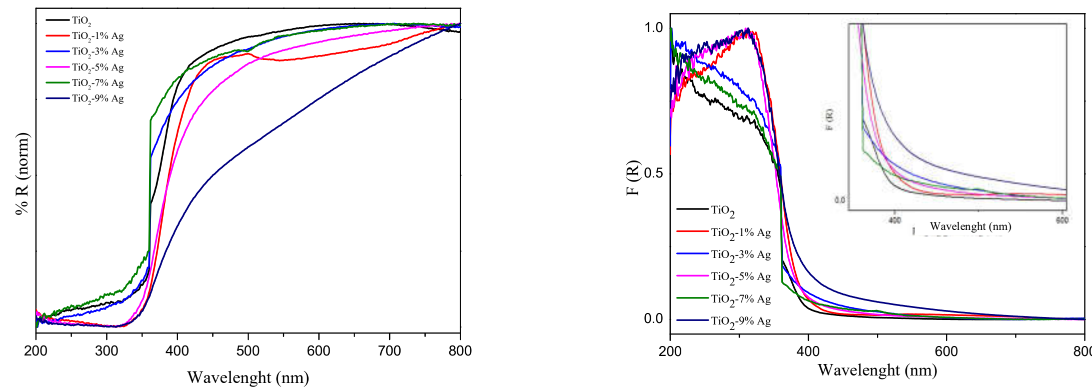

(a) (b)

FIGURE 3. DRS data of undoped TiO_2 and Ag-doped TiO_2 at 1-9 % a) Reflectance data (b) Absorption coefficient F(R) calculated by Kubelka Munk Function

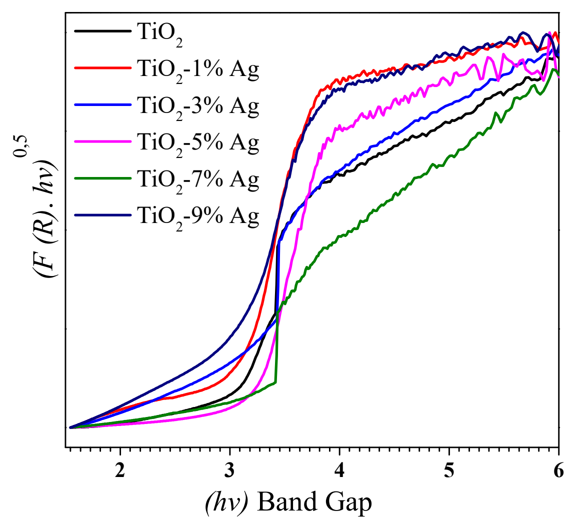

FIGURE 4. Indirect band gap energy of undoped and silver (Ag) doped TiO_2 photocatalyst at 1, 3, 5, 7, and 9% Silver (Ag)

TABLE 2. Antibacterial activity test against *E. coli* culture under UV light irradiation with a number of control bacteria is 4.6×10^8 cfu/mL

Photocatalyst Sample	Average Number of Colony (*cfu*/mL)	Viability (%)
Undoped TiO_2	3.42×10^8	25.65
1% Ag doped TiO_2	2.46×10^8	46.52
3% Ag doped TiO_2	1.22×10^8	73.47
5% Ag doped TiO_2	1.75×10^8	61.96
7% Ag doped TiO_2	6.65×10^6	98.55
9% Ag doped TiO_2	3.50×10^5	99.92

Percent viability test of all synthesized materials under UV radiation revealed that Ag-doped TiO_2 exhibited higher antibacterial activity than undoped TiO_2. Antibacterial activity raises as increasing of silver content. In visible radiation, each doped photocatalyst showed higher antibacterial activity compared to UV light irradiation. Among all doped materials, 5% of Ag-doped TiO_2 has the lowest activity both under UV and visible irradiation. It was contradictory with its activity without light irradiation. It might be related to the silver content in 5% of Ag-doped TiO_2 which was detected in its XRD pattern and the difference of reaction mechanism while light introduces into the reaction process. In this research, optimum activity was obtained from 9% Ag-doped photocatalyst which shown zero viability against *E. coli*.

TABLE 3. Antibacterial activity test against *E. coli* culture under Visible light irradiation with a number of control bacteria is 3.7×10^8 *cfu*/mL

Photocatalyst Sample	Average Number of Colony (*cfu*/mL)	Viability (%)
Undoped TiO_2	2.67×10^7	92.78
1% Ag doped TiO_2	2.40×10^7	93.51
3% Ag doped TiO_2	1.85×10^7	95.00
5% Ag doped TiO_2	2.85×10^7	92.29
7% Ag doped TiO_2	2.40×10^4	99.99
9% Ag doped TiO_2	0	100

SUMMARY

Silver doped TiO_2 photocatalysts were successfully synthesized at various dopant concentration (1-9%) using the sonochemical method. 9 % of Ag-doped TiO_2 possess the lowest reflectance, the highest absorption properties and the lowest band gap energy among all samples in this research. Silver dopant enhanced the antibacterial activity of anatase phase under ultraviolet and visible irradiation. 9% of silver dopant produces the optimum antibacterial activity against *E. coli* with zero viability under visible light irradiation.

ACKNOWLEDGEMENT

The authors gratefully acknowledge to Religion Ministry of Republic of Indonesia for BOPTN (Bantuan Operasional Perguruan Tinggi Negeri) in 2018 research grant.

REFERENCES

1. P. Pookmanee, I. Phiwchai, S. Yariya, R. Puntharod, S. Sangsrichan, J. Kittikul and S. Phanichphant, Mater. Sci. Forum **804** 209–212 (2015).
2. T. Ali, A. Ahmed, U. Alam, I. Uddin, P. Tripathi and M. Muneer, Mater. Chem. Phys. **212**, 325-335 (2018).
3. J. Lie, B. Xie, K. Xia, Y. Li, J. Han and C. Zhao, Materials **11**, 1403 (2018).
4. J. H .Bang and K. S. Suslick, Adv. Mater. **22,** 1039-1059 (2010).
5. N. Aini, R. Ningsih, D. Maulina, F. F. Lami' and S. N. Chasanah, in *International Conference on Advanded Material for Better Future*, IOP Conf. Ser. Mater. Sci. Eng. (IOP, 2018).
6. S. I. Mogal, V. G. Gandhi, M. Mishra, S. Tripathi, T. Shripathi, P. A. Joshi and D. O. Shah, Ind. Eng. Chem. Res. **53**, 5749-5758 (2014).
7. K. Gupta, R. P. Singh and A. Pandey, Beilstein J. Nanotechnol. **4**, 345–351 (2013).
8. G. Y. Nigussie, G. M. Tesfamariam, B. M. Tegegne, Y. A. Weldemichel, T. W. Gedreab, D. G. Gebrehiwot and G. E. Gebremichel, Int. J. Photoenergy **2018**, 345-349 (2018).